0026-895X/06/7003-786–792$20.00
MOLECULAR PHARMACOLOGY
Copyright © 2006 The American Society for Pharmacology and Experimental Therapeutics
Mol Pharmacol 70:786–792, 2006

Vol. 70, No. 3
26435/3134748
Printed in U.S.A.

ACCELERATED COMMUNICATION

Involvement of Neuronal Cannabinoid Receptor CB1 in Regulation of Bone Mass and Bone Remodeling

Joseph Tam, Orr Ofek, Ester Fride, Catherine Ledent, Yankel Gabet, Ralph Müller, Andreas Zimmer, Ken Mackie, Raphael Mechoulam, Esther Shohami, and Itai Bab

Bone Laboratory (J.T., O.O., Y.G., I.B.), Department of Medicinal Chemistry and Natural Products (R.M.) and Department of Pharmacology (E.S.), the Hebrew University of Jerusalem, Jerusalem, Israel; David R. Bloom Centre for Pharmacy, The Hebrew University School of Pharmacy, Jerusalem, Israel (E.S., R.M.); Department of Behavioral Sciences, College of Judea and Samaria, Ariel, Israel (E.F.); Institut de Recherche Interdisciplinaire en Biologie Humaine et Moléculaire, Université Libre de Bruxelles, Campus Erasme, Brussels, Belgium (C.L.); Institute for Biomedical Engineering, Swiss Federal Institute of Technology and University of Zürich, Zürich, Switzerland (R.M.); Laboratory of Molecular Neurobiology, Department of Psychiatry, University of Bonn, Bonn, Germany (A.Z.); and Departments of Anesthesiology and Physiology & Biophysics, University of Washington, Seattle, Washington (K.M.)

Received May 8, 2006; accepted June 13, 2006

ABSTRACT

The CB1 cannabinoid receptor has been implicated in the regulation of bone remodeling and bone mass. A high bone mass (HBM) phenotype was reported in CB1-null mice generated on a CD1 background (CD1$^{CB1-/-}$ mice). By contrast, our preliminary studies in *cb1*$^{-/-}$ mice, backcrossed to C57BL/6J mice (C57$^{CB1-/-}$ mice), revealed low bone mass (LBM). We therefore analyzed CB1 expression in bone and compared the skeletons of sexually mature C57$^{CB1-/-}$ and CD1$^{CB1-/-}$ mice in the same experimental setting. CB1 mRNA is weakly expressed in osteoclasts and immunoreactive CB1 is present in sympathetic neurons, close to osteoblasts. In addition to their LBM, male and female C57$^{CB1-/-}$ mice exhibit decreased bone formation rate and increased osteoclast number. The skeletal phenotype of the CD1$^{CB1-/-}$ mice shows a gender disparity. Female mice have normal trabecular bone with a slight cortical expansion, whereas male CD1$^{CB1-/-}$ animals display an HBM phenotype. We were surprised to find that bone formation and resorption are within normal limits. These findings, at least the consistent set of data obtained in the C57$^{CB1-/-}$ line, suggest an important role for CB1 signaling in the regulation of bone remodeling and bone mass. Because sympathetic CB1 signaling inhibits norepinephrine (NE) release in peripheral tissues, part of the endocannabinoid activity in bone may be attributed to the regulation of NE release from sympathetic nerve fibers. Several phenotypic discrepancies have been reported between C57$^{CB1-/-}$ and CD1$^{CB1-/-}$ mice that could result from genetic differences between the background strains. Unraveling these differences can provide useful information on the physiologic functional milieu of CB1 in bone.

The endogenous cannabinoids bind to and activate the CB1 and CB2 cannabinoid receptors. Both are seven-transmembrane domain receptors and they share 44% identity. They are coupled to the $G_{i/o}$ subclass of G-proteins and inhibit stimulated adenylyl cyclase activity (Rhee et al., 1997). CB1 is present in the brain and in peripheral neurons and accounts for most of the central nervous system actions of cannabinoid drugs and endocannabinoids (Herkenham et al., 1990; Zimmer et al., 1999). CB2 is found mainly in the immune system (Munro et al., 1993).

In vertebrates, bone mass and shape are determined by continuous remodeling consisting of the concerted and balanced action of osteoclasts, cells that resorb bone, and

This work was supported by National Institute on Drug Abuse grants DA9789 (to R.M.) and DA00286, DA11322 (to K.M.), and Israel Science Foundation (ISF) grants 482/01 and 4007/02-Bikura (to I.B. and E.S.). Purchase of the μCT system was supported in part by ISF grant 9007/01 (to I.B.).

J.T. and O.O. contributed equally to this article.

Article, publication date, and citation information can be found at http://molpharm.aspetjournals.org.
doi:10.1124/mol.106.026435.

ABBREVIATIONS: CD1$^{CB1-/-}$ mice, CB1-null mice generated on a CD1 background; C57$^{CB1-/-}$ mice, CB1-null mice generated on a C57BL/6J background; M-CSF, macrophage colony-stimulating factor; BV/TV, trabecular bone volume density.

osteoblasts, cells that form bone. Osteoporosis, the most prevalent degenerative disease in developed countries, results from impaired remodeling balance, which leads to bone loss and increased fracture risk. Bone remodeling is subject to central control through pathways that involve signaling by the hypothalamic receptors for leptin and neuropeptide Y (Ducy et al., 2000; Baldock et al., 2002), which are also associated with the regulation of endocannabinoid brain levels (Di Marzo et al., 2001). Along these lines, we have recently reported that 1) the peripheral CB2 cannabinoid receptor is normally expressed in osteoblasts, osteoclasts, and in their precursors; 2) mice deficient for CB2 have a low bone mass (LBM) phenotype; and 3) specific activation of CB2 attenuates ovariectomy-induced bone loss by restraining osteoclastogenesis and stimulating bone formation (Ofek et al., 2006).

Two mutant mouse lines with deficiency in the CB1 gene have been generated. In one line, backcrossed to C57BL/6J mice ($C57^{CB1-/-}$), almost the entire protein-encoding sequence was removed (Zimmer et al., 1999). In the other line, backcrossed to CD1 mice ($CD1^{CB1-/-}$), the N-terminal 233 codons of *cb1* were ablated (Ledent et al., 1999). Although both lines demonstrate a null mutation missing all the CB1 responsiveness to cannabinoid ligands, they display significant phenotypic discrepancies (Lutz, 2002; Hoffman et al., 2005). Regarding the skeleton, $CD1^{CB1-/-}$ mice have a high bone mass (HBM) phenotype, suggesting that activation of CB1 down-regulates bone mass (Idris et al., 2005). By contrast, our preliminary studies in $C57^{CB1-/-}$ mice pointed to a LBM phenotype occurring in the absence of functional CB1 receptors. These studies used different methods to characterize the skeletal phenotype. Hence, in an attempt to solve this critical discrepancy, we analyzed the expression and distribution of CB1 in bone and compared the skeletons of the $C57^{CB1-/-}$ and $CD1^{CB1-/-}$ mouse lines using identical methods, equipment, and expertise.

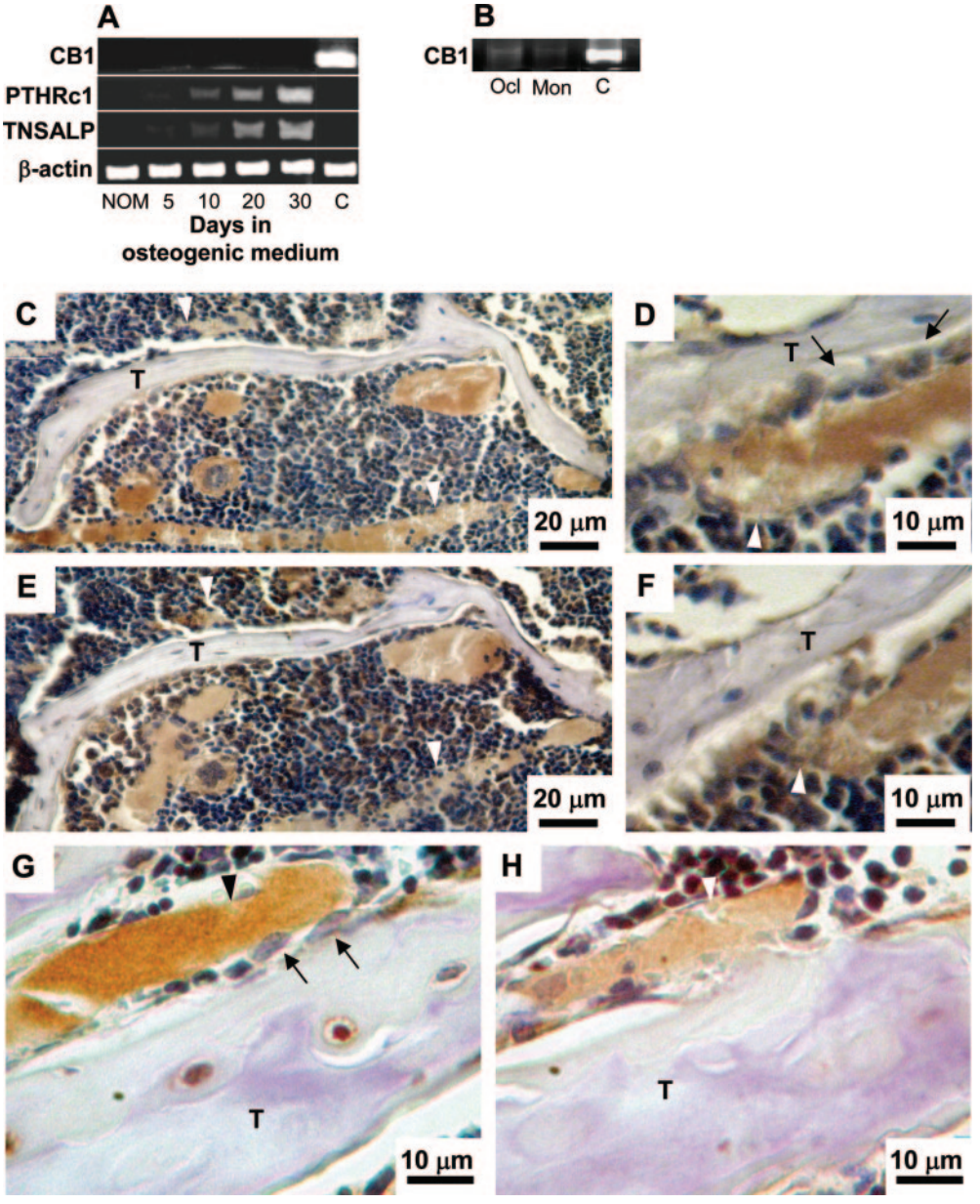

Fig. 1. CB1 is expressed in sympathetic nerve fibers in trabecular bone. A and B, RT-PCR analysis. A, bone marrow stromal cells undergoing osteoblastic differentiation in "osteogenic medium"; note absence of CB1-positive bands. PTHRc1, PTH receptor 1; TNSALP, tissue nonspecific alkaline phosphatase. NOM, cells grown for 20 days in nonosteogenic medium (negative control). Lane C, cerebellar mRNA (positive control). B, bone marrow-derived monocytic cells undergoing osteoclastogenesis in medium containing M-CSF and RANKL; Ocl, osteoclast-like tartrate-resistant acid phosphatase–positive multinucleated cells. Mon, undifferentiated monocytes. Lane C, cerebellar mRNA (positive control). Cells were derived from WT C57BL/6J mice. C–H, immunohistochemical staining in secondary spongiosa in distal femoral metaphysis from C57BL/6J (C–F) and CD1BL/6J (G and H) mice. C, D and G, anti-tyrosine hydroxylase antibodies; E, F, and H, consecutive sections stained with anti CB1 antibodies. T, bone trabeculae; arrows, osteoblasts; arrowheads, tyrosine hydroxylase-CB1 positive fibers. Hematoxylin counterstaining.

Materials and Methods

Animals. All animals in the study were 9- to 12-week-old mice. $C57^{CB1-/-}$ mice were generated as reported previously (Zimmer et al., 1999). We have crossed heterozygous animals of this line for at least 10 generations to WT C57BL/6J mice. Heterozygous animals from the last generation were then intercrossed to obtain congenic C57BL/6J mice that are homozygous for the respective mutation. $CD1^{CB1-/-}$ mice were generated by homologous recombination as described previously (Ledent et al., 1999). Heterozygous mice were bred for 17 generations on a CD1 background before generating the WT and *cb1*-null littermates used in this study. To study bone formation, newly formed bone was vitally labeled in mice intended for microcomputed tomographic (μCT)-histomorphometric analysis by the fluorochrome calcein (Sigma, St. Louis, MO), injected i.p. (15 mg/kg) 4 days and 1 day before sacrifice. The use of animals was approved by the Institutional Animal Care Committee of the Hebrew University of Jerusalem.

Immunohistochemistry. Mice were killed by transcardial perfusion of phosphate-buffered saline followed by 4% paraformaldehyde. The femora were dissected and further fixed with paraformaldehyde for 2 h at 4°C. The specimens were decalcified in 0.5 M EDTA, pH 7.4, and embedded in paraffin. For immunohistochemical analysis, serial 5-μm frontal sections were reacted with anti-tyrosine hydroxylase (TH) (Chemicon, Temecula, CA) or anti-CB1 antibodies (Nyíri et al., 2005). Further processing was carried out using the SuperPicture polymer detection Kit (Zymed Laboratories, South San Francisco, CA) according to the manufacturer instructions.

Cell Cultures and mRNA Analysis. Primary bone marrow stromal cell cultures from WT adult femoral and tibial diaphyseal bone marrow were established as described previously. For testing CB1 expression, the cells were grown in osteogenic medium (Ofek et al., 2006). Bone marrow-derived osteoclastogenic cultures were established from Ficoll-separated monocytic precursors and grown for 5 to 6 days in medium containing macrophage colony-stimulating factor (M-CSF) and RANK ligand (RANKL; R&D Systems, Minneapolis, MN) (Ofek et al., 2006). Total RNA was extracted from the cells, purified, and reverse-transcribed using routine procedures. The following primers were used for PCR: CB1, sense: 5′-TGGTGTATGATGTCTTTGGG-3′, antisense: 5′-ATGCTGGCTGTGTTATTGGC-3′; tissue nonspecific alkaline phosphatase, sense: 5′-GACACAAGCATTCCCACTAT-3′, antisense: 5′-ATCAG-CAGTAACCACAGTCA-3′; parathyroid hormone receptor I, sense: 5′-CAAGAAGTGGATCATCCAGGT-3′, antisense: 5′-GCTGCTACTCCCACTTCGTGCTTT-3′; and β-actin, sense, 5′-GAGACCTTCAACACCCCAGCC-3′; antisense, 5′-GGCCATCTCTTGCTCGAAGTC-3′.

μCT Analysis. Whole femora were examined by a μCT system (μCT 40; SCANCO Medical, Bassersdorf, Switzerland) as reported recently (Bajayo et al., 2005; Ofek et al., 2006). Scans were performed at a resolution of 20 μm in all three spatial dimensions. Morphometric parameters were determined as reported previously (Kram et al., 2006). Trabecular and cortical bone parameters were measured in metaphyseal and mid-diaphyseal segments, respectively.

Histomorphometry. After μCT image acquisition, the specimens were embedded undecalcified in Technovit 9100 (Heraeus). Longitu-

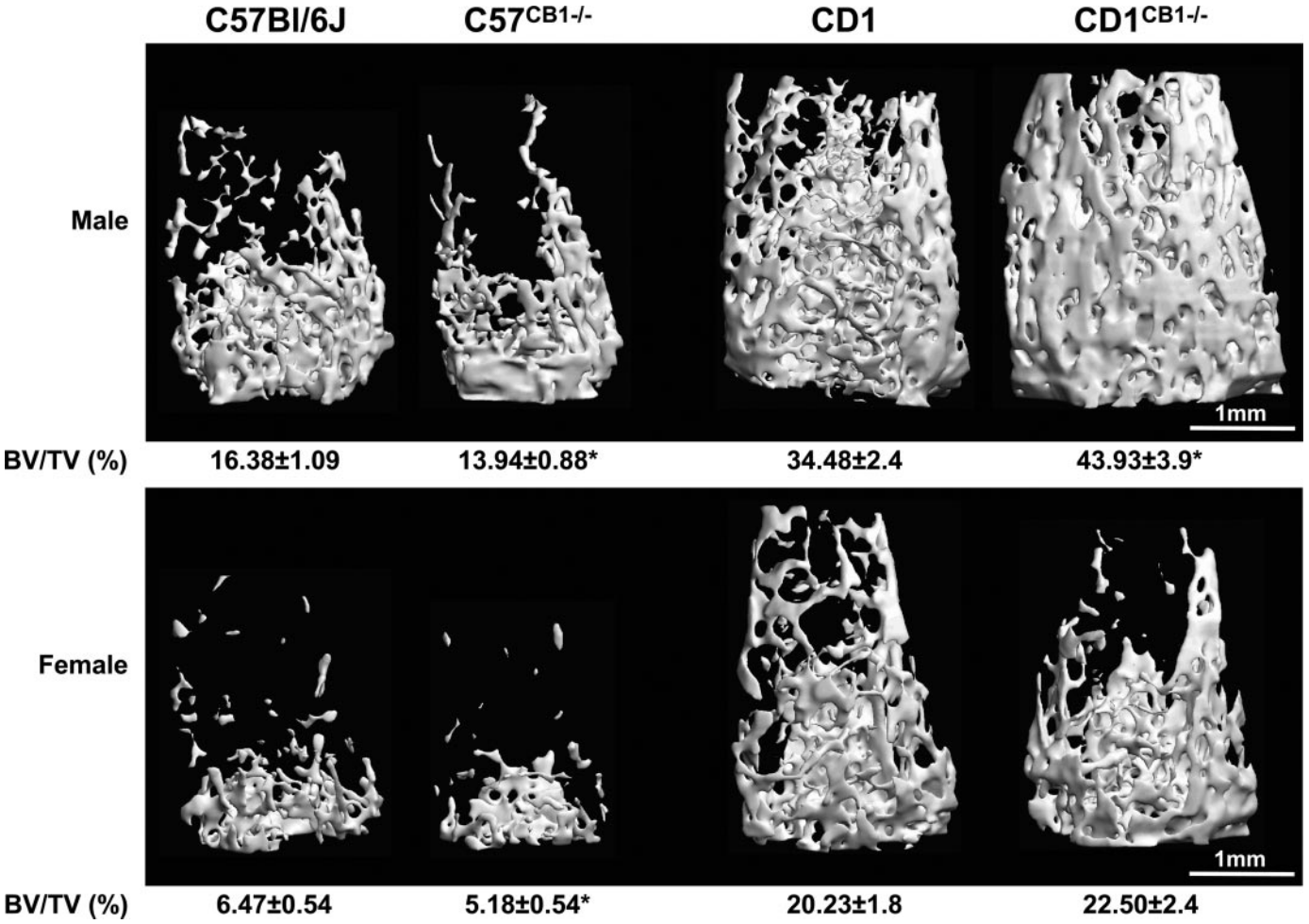

Fig. 2. Bone mass phenotype in CB1-null mice. Tri-dimensional μCT images of distal femoral metaphysial trabecular bone from mice with median BV/TV values. Quantitative data are mean ± S.E.M. obtained in 16 $C57^{CB1-/-}$ and 16 WT C57BL/6J mice per gender, six $CD1^{CB1-/-}$ and six WT CD1 male mice and 20 $CD1^{CB1-/-}$ and 20 WT CD1 female mice. *, $P < 0.05$.

dinal sections through the midfrontal plane were left unstained for dynamic histomorphometry, based on the vital calcein double labeling. To identify osteoclasts, consecutive sections were stained for tartrate-resistant acid phosphatase. Parameters were determined according to a standardized nomenclature (Parfitt et al., 1987).

Statistical Analysis. Differences between *cb1*$^{-/-}$ and WT mice were analyzed with the use of the Student's *t* test.

Results and Discussion

Expression of CB1 in Bone. mRNA analyses were carried out in cells derived from WT C57BL/6J mice. Unlike the expression of CB2, which is absent in undifferentiated bone marrow stromal cells but increases progressively when these cells undergo osteoblastic differentiation (Ofek et al., 2006), we were unable to identify CB1 mRNA transcripts in either undifferentiated or differentiated stromal cells, even after 40 PCR cycles (Fig. 1A). Monocytic osteoclast precursors from these mice also did not show CB1 expression. However, a weak signal was present when these cells underwent osteoclastogenesis with M-CSF and RANKL (Fig. 1B).

Bone, especially trabecular bone, is densely innervated by sympathetic fibers (Serre et al., 1999; Mach et al., 2002). These fibers release norepinephrine, thus potently mediating central signals that restrain bone formation and stimulate bone resorption (Elefteriou et al., 2005). Because CB1 is expressed in such nerve fibers elsewhere (Schlicker and Kathmann, 2001), we further explored its presence in bone sympathetic nerve fibers. Indeed, immunohistochemical analysis using the sympathetic marker TH (Bjurholm et al., 1988) confirmed the occurrence of a network of TH-positive fibers in the intertrabecular spaces of cancellous bone in both C57BL/6J and CD1 mice (Fig. 1, C and G). The fibers were close to the bone trabeculae with terminal nerve processes penetrating the osteoblast palisades, thus being in intimate proximity to these cells (Fig. 1, D and G). Consecutive histological sections show CB1 immunoreactivity of the same nerve fibers (Fig. 1, E, F, and H), indicating the presence of CB1 receptors in sympathetic fibers that innervate the trabecular bone. This CB1 immunoreactivity was missing in the CB1-null mice (data not shown).

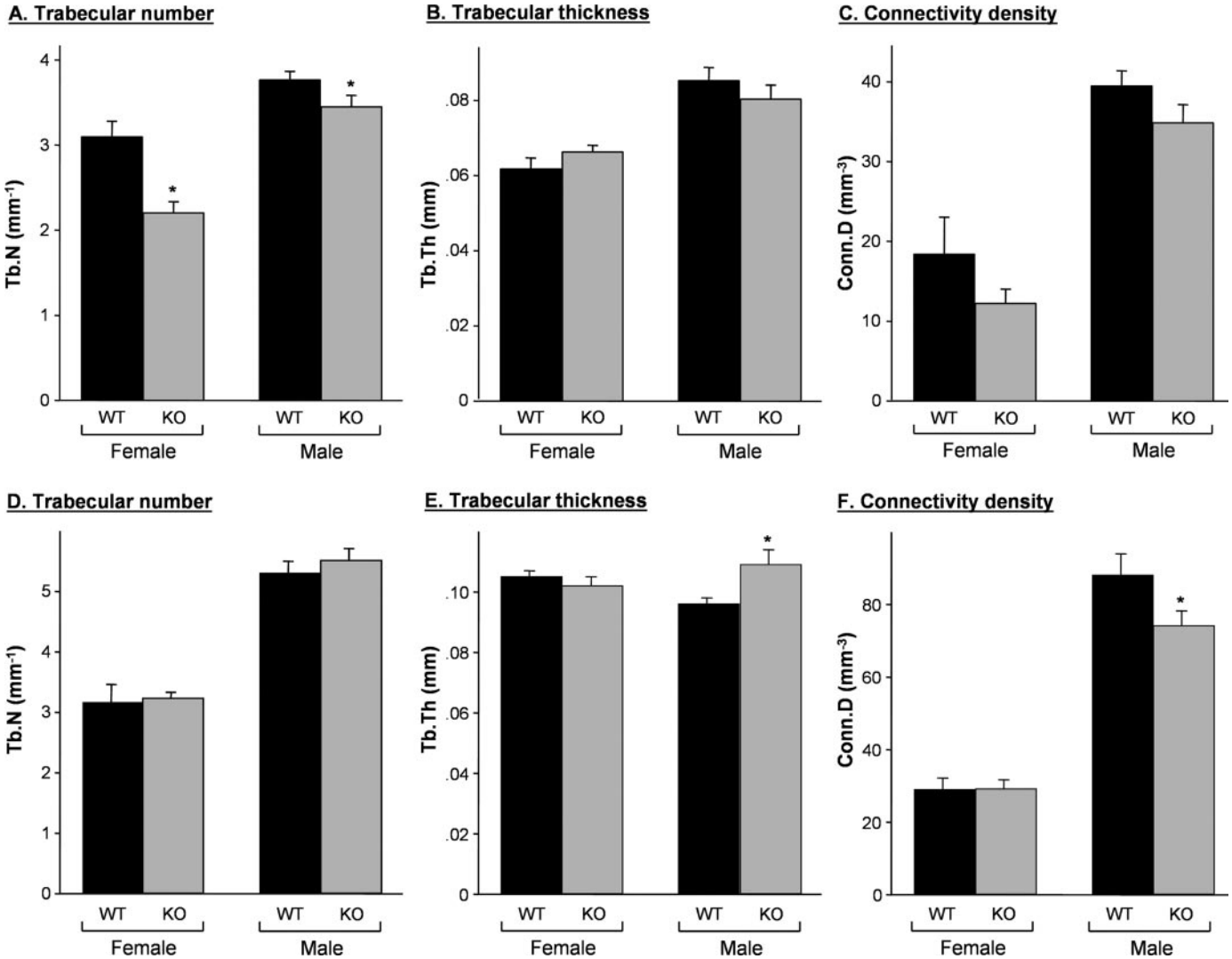

Fig. 3. μCT-based structural morphometric parameters in secondary spongiosa of distal femoral metaphysis of CB1-null mice. A–C, C57$^{CB1-/-}$ mice and their WT C57BL/6J control mice; D–F, CD1$^{CB1-/-}$ mice and their WT CD1 control mice. A and D, trabecular number. B and E, trabecular thickness. C and F, trabecular connectivity. Data are mean ± S.E.M. obtained in 16 C57$^{CB1-/-}$ and 16 WT C57BL/6J mice per gender, six CD1$^{CB1-/-}$ and six WT CD1 male mice and 20 CD1$^{CB1-/-}$ and 20 WT CD1 female mice. *, $P < 0.05$.

Skeletal Phenotype of CB1-Null Mice. Our results demonstrate that the background WT strains, in which the C57$^{CB1-/-}$ and CD1$^{CB1-/-}$ mouse lines had been established, display vast differences in both trabecular and cortical bone mass. More importantly, *cb1* inactivation in these lines resulted in opposing skeletal effects (Figs. 2–4).

Compared with their WT control mice, both male and female C57$^{CB1-/-}$ mice exhibited low bone mass (LBM) phenotype characterized by a lower density of their trabecular network. The trabecular bone volume density (BV/TV) in female and male null mice was 20 and 15% lower than that of WT C57BL/6J control mice, respectively (Fig. 2). Apparently, the lower BV/TV in the C57$^{CB1-/-}$ mice resulted from decreases in the trabecular number (Fig. 3A) without changes in the trabecular thickness (Fig. 3B). The trabecular connectivity density, a parameter measuring the structural integrity of the trabecular network (Stampa et al., 2002), was also decreased in these animals (Fig. 3C) but did not reach statistical difference. In addition, both the diaphyseal shaft diameter and medullary cavity diameter were narrower in the C57$^{CB1-/-}$ mice (Fig. 4, A and B), with unchanged cortical thickness (Fig. 4C).

By contrast, the CD1$^{CB1-/-}$ skeletal phenotype showed a marked gender bias. The trabecular bone, the main skeletal compartment affected in osteoporosis, appeared normal in female CD1$^{CB1-/-}$ mice (Figs. 2 and 3, D–F). Male CD1$^{CB1-/-}$ mice had a pronounced HBM phenotype demonstrating 27.5% increase in trabecular BV/TV (Fig. 2) accompanied by increased trabecular thickness (Fig. 3E) and slightly decreased connectivity density (Fig. 3F). The female CD1$^{CB1-/-}$ diaphysis was mildly abnormal, exhibiting cortical expansion portrayed as increases in both diaphyseal shaft diameter and medullary cavity diameter (Fig. 4, D and E). The male CD1$^{CB1-/-}$ diaphysis appeared normal (Fig. 4, D–F).

To gain further insight into the processes leading to the LBM phenotype in C57$^{CB1-/-}$ mice, we analyzed their bone remodeling. Consistent with the results of the structural μCT parameters, the histomorphometric analysis demonstrated that the LBM in these mice is associated with unbalanced bone remodeling. The bone formation rate was markedly decreased in both female and male mice (Fig. 5A), mainly because of a decrease in mineral appositional rate, a surrogate of osteoblast activity (Fig. 5B), inasmuch

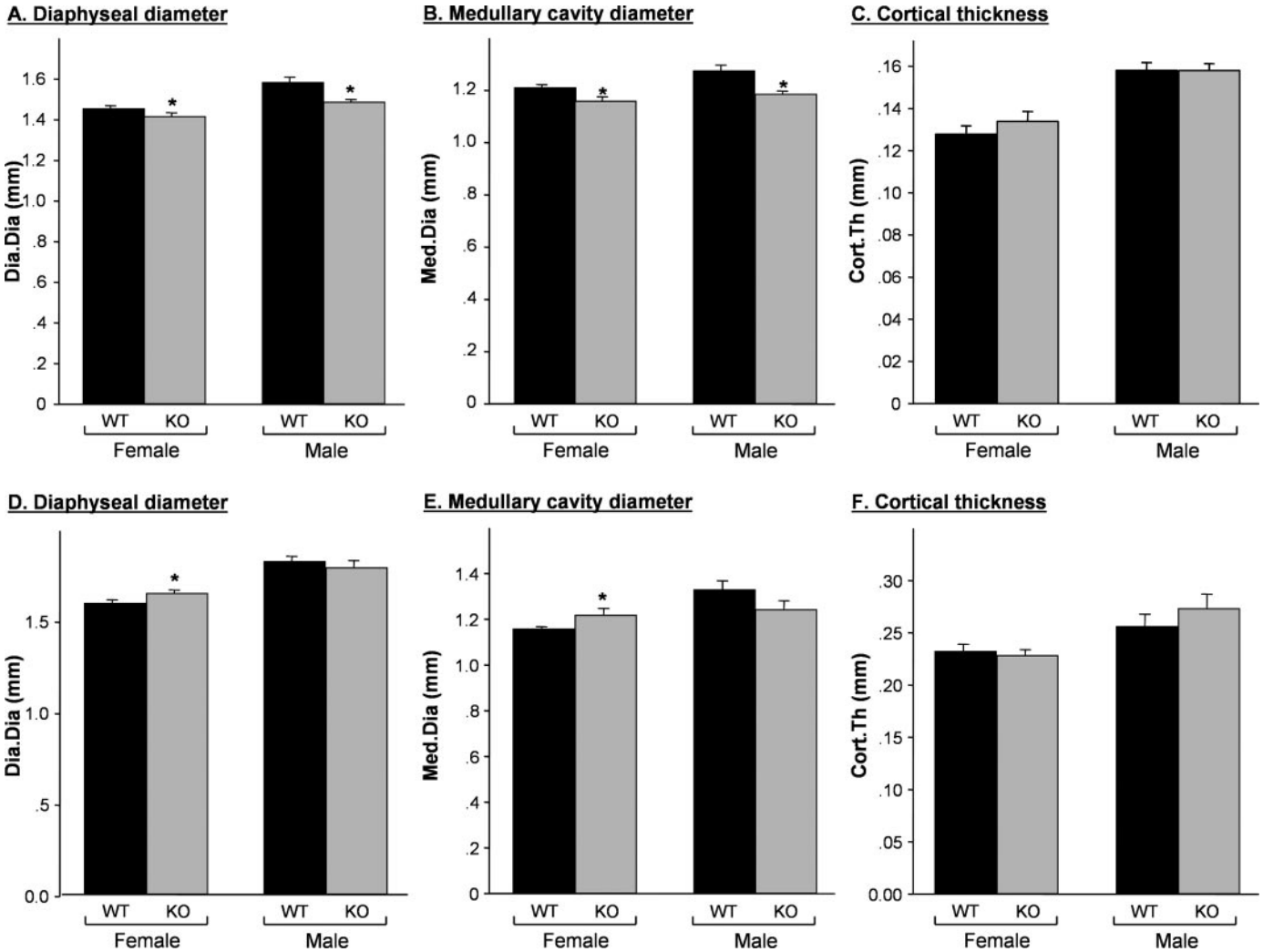

Fig. 4. μCT-based measurements of diaphyseal dimensions in CB1-null mice. A–C, C57$^{CB1-/-}$ mice and their WT C57BL/6J control mice; D–F, CD1$^{CB1-/-}$ mice and their WT CD1 control mice. A and D, overall mid-diaphyseal diameter. B and E, mid-diaphyseal medullary cavity diameter. C and F, cortical thickness. Data are mean ± S.E.M. obtained in 16 C57$^{CB1-/-}$ and 16 WT C57BL/6J mice per gender, six CD1$^{CB1-/-}$ and six WT CD1 male mice and 20 CD1$^{CB1-/-}$ and 20 WT CD1 female mice. *, $P < 0.05$.

as the mineralizing perimeter, a surrogate of osteoblast number, remains unchanged (Fig. 5C). The osteoclast number was increased, significantly in female mice and insignificantly in male mice (Fig. 5D). We were surprised to find no significant differences in bone remodelling parameters between the $CD1^{CB1-/-}$ mice and their WT control mice, even not in male mice (Table 1). Together, these results suggest that in the C57BL/6J mice, CB1 signaling positively regulates trabecular bone mass and radial diaphyseal growth by up-regulating bone formation and down-regulating bone resorption. The absence of significant changes in bone remodeling parameters of the male $CD1^{CB1-/-}$ mice suggests that CB1 in these animals is associated only with the accrual of peak bone mass, which occurs at a younger age than that studied here. Apparently, the LBM phenotype is exhibited in the $C57^{CB1-/-}$ mice consequent to a decrease in bone formation and increase in bone resorption attributable to the absence of sympathetic CB1, which normally inhibits norepinephrine release (Ishac et al., 1996).

Although either genetic modification leads to a null mutation missing all CB1 responsiveness to its ligands, the occurrence of phenotypic differences is not entirely surprising, inasmuch as these mouse lines exhibit other substantial discrepancies ranging from nociceptive perception to locomotor activity, life expectancy, and embryo implantation (Lutz, 2002). Furthermore, at least to some extent, skeletal dissimilarity between the $C57^{CB1-/-}$ and $CD1^{CB1-/-}$ mice could be expected from the differences in bone mass and structure observed between the WT CD1 and C57BL/6J background strains. More surprising is the gender bias portrayed by the

TABLE 1

Trabecular histomorphometric bone remodeling parameters of male $CD1^{CB1-/-}$ mice

Data are mean ± S.E. in six male CD1 mice.

Genotype	MAR	Min.Peri	BFR	N.Oc/BS
	$\mu m/day$	%	$mm^3/mm^2/day$	mm^{-1}
$CD1^{CB1-/-}$	2.82 ± 0.19	54.5 ± 5.91	1.55 ± 0.22	2.71 ± 0.31
WT	2.73 ± 0.14	46.7 ± 2.53	1.27 ± 0.04	2.49 ± 0.49

MAR, mineral appositional rate; Min.Peri, mineralizing perimeter; BFR, bone formation rate; N.Oc/BS, osteoclasts number; WT, wild-type CD1 mice.

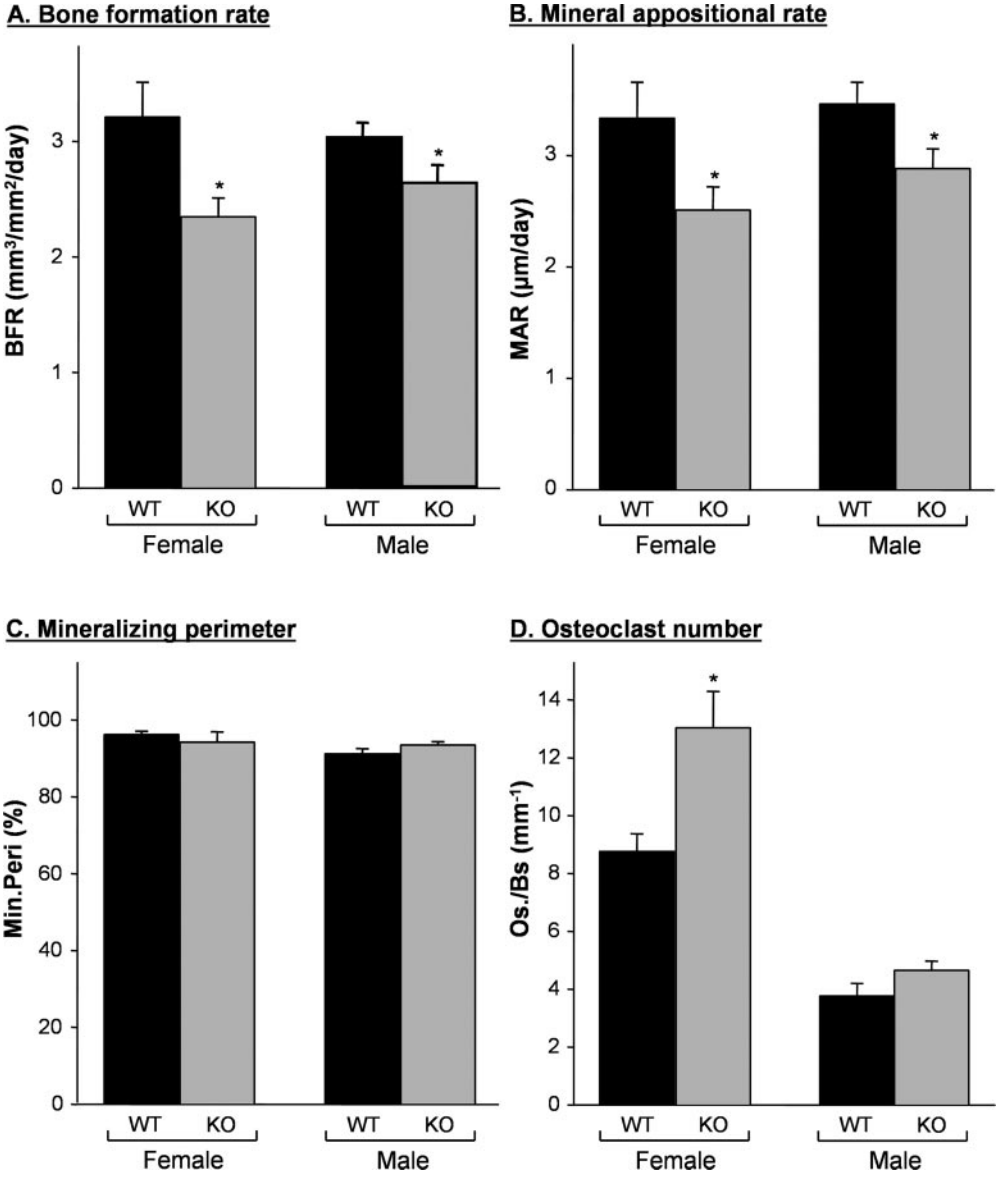

Fig. 5. Histomorphometric bone remodeling parameters in secondary spongiosa of distal femoral metaphysis of $C57^{CB1-/-}$ mice. A, bone formation rate. B, mineral appositional rate. C, mineralizing perimeter. D, osteoclast number. Data are mean ± S.E.M. obtained in eight mice per condition. *, $P < 0.05$.

$CD1^{CB1-/-}$ mice and the absence of changes in bone remodeling in male animals that could explain their HBM. Although a HBM phenotype, unaccompanied by changes in bone remodeling, was reported previously (Idris et al., 2005), it is unclear to us whether it was assigned to male mice, female mice, or both.

Despite the differences between the two mouse lines, the present findings [especially the consistency in $C57^{CB1-/-}$ mice presented by 1) CB1 expression in bone; 2) LBM; and 3) changes in skeletal turnover parameters] suggest a role for sympathetic CB1 in the control of bone remodeling and bone mass. In fact, unraveling the genetic differences between the C57BL/6J and CD1 strains, as well as the genetic basis for the gender discrimination within the $CD1^{CB1-/-}$ mouse line, can provide useful information on the physiologic functional milieu of CB1 in bone. Until an explanation for the skeletal (and possibly other) differences between the $C57^{CB1-/-}$ and $CD1^{CB1-/-}$ mice is found, it is our approach that only experimental trends shared by both mouse lines should be considered.

Acknowledgments

We thank Olga Lahat, Malka Attar, Meirav Fogel, and Dr. Ravit Birenboim for expert assistance.

References

Bajayo A, Goshen I, Feldman S, Csernus V, Iverfeldt K, Shohami E, Yirmiya R, and Bab I (2005) Central IL-1 receptor signaling regulates bone growth and mass. *Proc Natl Acad Sci USA* **102:**12956–12961.

Baldock PA, Sainsbury A, Couzens M, Enriquez RF, Thomas GP, Gardiner EM, and Herzog H (2002) Hypothalamic Y2 receptors regulate bone formation. *J Clin Investig* **109:**915–921.

Bjurholm A, Kreicbergs A, Terenius L, Goldstein M, and Schultzberg M (1988) Neuropeptide Y-, tyrosine hydroxylase- and vasoactive intestinal polypeptide-immunoreactive nerves in bone and surrounding tissues. *J Auton Nerv Syst* **25:**119–125.

Di Marzo V, Goparaju SK, Wang L, Liu J, Batkai S, Jarai Z, Fezza F, Miura GI, Palmiter RD, Sugiura T, et al. (2001) Leptin-regulated endocannabinoids are involved in maintaining food intake. *Nature (Lond)* **410:**822–825.

Ducy P, Amling M, Takeda S, Priemel M, Schilling AF, Beil FT, Shen J, Vinson C, Rueger JM, and Karsenty G (2000) Leptin inhibits bone formation through a hypothalamic relay: a central control of bone mass. *Cell* **100:**197–207.

Elefteriou F, Ahn JD, Takeda S, Starbuck M, Yang X, Liu X, Kondo H, Richards WG, Bannon TW, Noda M, et al. (2005) Leptin regulation of bone resorption by the sympathetic nervous system and CART. *Nature (Lond)* **434:**514–520.

Herkenham M, Lynn AB, Little MD, Johnson MR, Melvin LS, de Costa BR, and Rice KC (1990) Cannabinoid receptor localization in brain. *Proc Natl Acad Sci USA* **87:**1932–1936.

Hoffman AF, Macgill AM, Smith D, Oz M, and Lupica CR (2005) Species and strain differences in the expression of a novel glutamate-modulating cannabinoid receptor in the rodent hippocampus. *Eur J Neurosci* **22:**2387–2391.

Idris AI, van't Hof RJ, Greig IR, Ridge SA, Baker D, Ross RA, and Ralston SH (2005) Regulation of bone mass, bone loss and osteoclast activity by cannabinoid receptors. *Nat Med* **11:**774–779.

Ishac EJ, Jiang L, Lake KD, Varga K, Abood ME, and Kunos G (1996) Inhibition of exocytotic noradrenaline release by presynaptic cannabinoid CB1 receptors on peripheral sympathetic nerves. *Br J Pharmacol* **118:**2023–2028.

Kram V, Zcharia E, Yacoby-Zeevi O, Metzger S, Chajek-Shaul T, Gabet Y, Muller R, Vlodavsky I, and Bab I (2006) Heparanase is expressed in osteoblastic cells and stimulates bone formation and bone mass. *J Cell Physiol* **207:**784–792.

Ledent C, Valverde O, Cossu G, Petitet F, Aubert JF, Beslot F, Bohme GA, Imperato A, Pedrazzini T, Roques BP, et al. (1999) Unresponsiveness to cannabinoids and reduced addictive effects of opiates in CB1 receptor knockout mice. *Science (Wash DC)* **283:**401–404.

Lutz B (2002) Molecular biology of cannabinoid receptors. *Prostaglandins Leukot Essent Fatty Acids* **66:**123–142.

Mach DB, Rogers SD, Sabino MC, Luger NM, Schwei MJ, Pomonis JD, Keyser CP, Clohisy DR, Adams DJ, O'Leary P, et al. (2002) Origins of skeletal pain: sensory and sympathetic innervation of the mouse femur. *Neuroscience* **113:**155–166.

Munro S, Thomas KL, and Abu-Shaar M (1993) Molecular characterization of a peripheral receptor for cannabinoids. *Nature (Lond)* **365:**61–65.

Nyíri G, Cserep C, Szabadits E, Mackie K, and Freund TF (2005) CB1 cannabinoid receptors are enriched in the perisynaptic annulus and on preterminal segments of hippocampal GABAergic axons. *Neuroscience* **136:**811–822.

Ofek O, Karsak M, Leclerc N, Fogel M, Frenkel B, Wright K, Tam J, Attar-Namdar M, Kram V, Shohami E, et al. (2006) Peripheral cannabinoid receptor, CB2, regulates bone mass. *Proc Natl Acad Sci USA* **103:**696–701.

Parfitt AM, Drezner MK, Glorieux FH, Kanis JA, Malluche H, Meunier PJ, Ott SM, and Recker RR (1987) Bone histomorphometry: standardization of nomenclature, symbols, and units. Report of the ASBMR Histomorphometry Nomenclature Committee. *J Bone Miner Res* **2:**595–610.

Rhee MH, Vogel Z, Barg J, Bayewitch M, Levy R, Hanus L, Breuer A, and Mechoulam R (1997) Cannabinol derivatives: binding to cannabinoid receptors and inhibition of adenylylcyclase. *J Med Chem* **40:**3228–3233.

Schlicker E and Kathmann M (2001) Modulation of transmitter release via presynaptic cannabinoid receptors. *Trends Pharmacol Sci* **22:**565–572.

Serre CM, Farlay D, Delmas PD, and Chenu C (1999) Evidence for a dense and intimate innervation of the bone tissue, including glutamate-containing fibers. *Bone* **25:**623–629.

Stampa B, Kuhn B, Liess C, Heller M, and Gluer CC (2002) Characterization of the integrity of three-dimensional trabecular bone microstructure by connectivity and shape analysis using high-resolution magnetic resonance imaging in vivo. *Top Magn Reson Imaging* **13:**357–363.

Zimmer A, Zimmer AM, Hohmann AG, Herkenham M, and Bonner TI (1999) Increased mortality, hypoactivity, and hypoalgesia in cannabinoid CB1 receptor knockout mice. *Proc Natl Acad Sci USA* **96:**5780–5785.

Address correspondence to: Prof. Itai Bab, Bone Laboratory, the Hebrew University of Jerusalem, PO Box 12272, Jerusalem 91120, Israel. E-mail: babi@cc.huji.ac.il